Positronium formation from positron impact on hydrogen and helium targets

T. C. Naginey and Eric W. Stacy
Physics Department, Old Dominion University, Norfolk, Virginia 23529, USA

B. B. Pollock
Lawrence Livermore National Laboratory, Livermore, California 94550, USA

H. R. J. Walters
Department of Applied Mathematics and Theoretical Physics, The Queen's University, Belfast BT7 1NN, United Kingdom

Colm T. Whelan
Physics Department, Old Dominion University, Norfolk, Virginia 23529, USA and Lawrence Livermore National Laboratory, Livermore, California 94550, USA

(Received 27 March 2014; published 6 June 2014)

Charge-exchange cross sections are presented for collisions of positrons with hydrogen and neutral and singly ionized helium targets using a variant of the classical trajectory Monte Carlo approach. As a check on the method a comparison is made with the corresponding proton results. An extended error analysis is presented. Reasonable agreement with available experimental data is found, and the charge-exchange cross section for positrons on He^+ is predicted.

DOI: 10.1103/PhysRevA.89.062704 PACS number(s): 34.80.Uv, 34.10.+x, 31.15.−p, 52.20.Hv

I. BACKGROUND

The understanding of positron processes is an area of heightened interest in many branches of physics. In particular their significance has long been recognized in astrophysics. Positrons are produced at a tremendous rate at the center of the galaxy; estimates from studies of the 511-keV γ-ray line suggest a rate of $\approx 10^{43}$ e^+/s [1]. Despite 30 years of intense effort the main source of these positrons has not been identified (for a recent review see [2,3]). Further, a knowledge of the ratio of the singlet-state and triplet-state photon fluxes would be a valuable diagnostic for understanding the physical conditions in a wide range of astrophysical sources, such as type Ia supernovae, microquasars, and x-ray binaries [2,4]; a direct observation of positronium would be an important contribution to the physical understanding of jets escaping from quasars into the interstellar medium [5]. A study of 3γ versus 2γ emission would allow the determination of the temperature and density of the plasma in solar flares [6]. It is only recently that experimental progress has been made towards the goal of producing intense beams of positrons in the laboratory; Chen and collaborators [7,8] have succeeded in producing record amounts of positrons (they estimate one million particles per laser shot), and positrons have been observed in experiments by firing wakefield accelerated electrons into solid targets [9]. These new laser-driver approaches open up the possibility that superintense positron sources will become a reality in the near future and, consequently, could be used as diagnostic tools and for the performance of significant experiments. Our own particular interest is in the possibility of using positronium formation as a probe of plasma properties and studying the positronium fraction in laboratory-produced plasmas [4,10]. In astrophysical situations the plasmas of interest consist of hydrogen and helium atoms and ions. In this paper we will focus on positron collisions with neutral hydrogen and helium as well as with singly ionized helium. Our goal is to produce cross sections of sufficient accuracy which could be used in modeling positronium formation in collisions between positrons and atoms or ions. We are fortunate to have available high-quality charge-exchange cross-sectional experimental data for positron-neutral atom collisions [11], but there are no experiments for collisions between positrons and ions. Our approach has been to use the well-known classical trajectory Monte Carlo (CTMC) method for both the positron and proton projectiles. Our strategy is to benchmark our theoretical approach for proton impact charge exchange before applying it to the equivalent positron process. Unless otherwise stated, atomic units where $e = m = \hbar = a_0 = 1$ are used.

II. CLASSICAL TRAJECTORY MONTE CARLO APPROACH

The CTMC approach [12–15] is in essence a computer experiment. In this method exact classical dynamics are performed on trajectories whose initial conditions are chosen from a classical ensemble. The initial energy of the target atom is fixed from known quantum-mechanical energies, e.g., $E_0 = -0.5$ a.u. for hydrogen. It is assumed that the initial coordinates and momenta are uniformly distributed in phase space on this energy shell; this condition effectively defines the classical microcanonical distribution. The quantum-mechanical probability distribution in momentum space for the nth level of a one-electron atom [16] is the identical distribution which follows from the classical microcanonical distribution [12]. The classical nature of the CTMC approach means that there is capture into all states of the positronium atom. The accuracy we can expect from the CTMC method is open to dispute; certainly, at low impact energies near threshold one would expect that the electron will tunnel through the potential barrier it encounters. This is a quantum-mechanical process and therefore is entirely absent from the CTMC. At the other

extreme of very high energies all classical calculations have the wrong asymptotic behavior [12,17].

A. Errors

There are three main sources of error inherent in the CTMC method: (i) the error due to beginning and ending each simulated scattering event (or "run") with the projectile and the target at a finite distance from each other, (ii) the error due to the nonzero step length in the numerical Runge-Kutta integration of the equations of motion, and (iii) statistical error, which decreases with the total number of runs evaluated. Errors (i) and (ii) can be controlled explicitly by two parameters in the input of the CTMC program, γ and ϵ, while error (iii) can only be reduced by increasing the number of runs that our program cycles through for each incident energy.

B. Error parameters γ and ϵ

The value of the input parameter γ is approximately the ratio of the major diameter of the target atom to the initial distance between the projectile and target. Its value is selected by the user and determines the starting and ending times of each run through the relationships

$$\gamma = \frac{|Z_n|}{E_i D_i(t_-)} = \frac{|Z_p|}{E_f D_f(t_+)} \tag{1}$$

defined in [13], where Z_p, Z_n are the charges of the projectile and target nucleus, respectively, E_i and E_f are the binding energies of the initially bound target atom and the finally bound "atom" resulting from the charge transfer, $D_i(t_-)$ is the initial distance between the CM of the projectile and target atom at the beginning of the run, and $D_f(t_+)$ is the final distance between the projectile and nucleus at the end of the run. Since the Coulomb interaction before time t_- and after time t_+ is neglected, it would seem that the smaller the choice of γ is, the more accurate our simulation will be. However, as we shrink γ, we will need more steps in the numerical integration (assuming constant step size), and the buildup of error due to the finite step size of the Runge-Kutta method can become unmanageable. In order to control this a second error parameter, ϵ, is introduce to fix the step length of the numerical integration Δt through the following relationship:

$$\frac{\epsilon^2}{(\Delta t)^2} = \left[\left(\frac{v}{r}\right)^2 + \frac{\epsilon}{2}\left|\frac{\dot{\mathbf{v}}}{r}\right|\right], \tag{2}$$

where v and r are the relative velocity and distance between two particles. Since there are three particles under consideration, Δt is actually computed by combining the above expressions for each two-particle interaction. It is worth noting that the step size varies with the product of the charges Z_p, Z_n. For a fixed value of ϵ, the step size will be smaller when the charge on either particle is increased; consequently, the error due to finite step size will be larger if either charge is greater than 1. We measure these errors by measuring how badly the program violates conservation of energy. This is done by evaluating the total energy of all three particles at the beginning and end of each run. There are four quantities of interest here: the actual initial energy of all particles E_i, the initial energy neglecting the interaction between the projectile and target $E_{i,\mathrm{mod}}$, the actual final energy of all particles E_f, and the final energy neglecting the interaction between the new atom and the nucleus, in the case of capture, $E_{f,\mathrm{mod}}$. Each of these four quantities is evaluated for each event. We can measure the error due to starting and ending the collision at finite times by the differences $|E_i - E_{i,\mathrm{mod}}|$ and $|E_f - E_{f,\mathrm{mod}}|$. Likewise, we can measure the error due to finite step size in the numerical integration using the difference $|E_i - E_f|$; if the integration were 100% accurate, this difference would always be zero. We measured the average and the standard deviation of these differences each time the program is run. If for a given impact energy the error exceeds a certain limit, the result is not used. For positron projectiles, this limit is that the average of the absolute difference between E_i and E_f plus the standard deviation of this difference should be less than 35% of the impact energy of the positron:

$$\overline{|E_i - E_f|} + \sigma_{|E_i - E_f|} < 0.35 T_{e^+}. \tag{3}$$

Enforcing this inequality can necessitate accepting quite large statistical errors at low energies for positron impact processes. It is well known from numerical treatments of the Kepler problem in celestial mechanics that standard integrating methods such as the Runge-Kutta technique can give rise to similar violations in energy conservation [18,19].

C. Statistical error

The statistical error associated with the cross sections calculated by the CTMC program is given by the binomial distribution [12,13]. Let us denote a particular event (such as charge transfer) by q and the number of occurrences of that event by n_q. Then, letting n be the total number of runs, the statistical error associated with the cross section for q is given by

$$\sigma_q \left(\frac{n - n_q}{n_q n}\right)^{\frac{1}{2}}, \tag{4}$$

where σ_q is the "experimental estimate" of the cross section for a particular property of the final state, q, and is defined by

$$\sigma_q = \frac{n_q}{n} \pi a_{\max}^2 \tag{5}$$

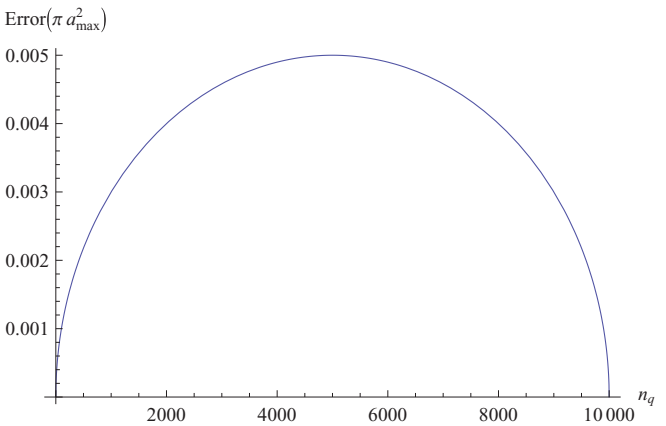

FIG. 1. (Color online) Statistical error as a function of n_q, with $n = 10\,000$.

where $a_{\max}$ is the radius beyond which event q no longer occurs. The maximum statistical error is then

$$\frac{1}{2\sqrt{n}}\pi a_{\max}^2 \tag{6}$$

and occurs when $n_q = \frac{1}{2}n$. Figure 1 is a plot of how the error varies with n_q for a typical CTMC calculation of 10 000 runs.

III. RESULTS

A. Hydrogen

Although for a one-electron atom the microcanonical distribution returns the quantum-mechanical momentum distribution, the spatial distribution of the charge is not as good. To correct for this Cohen [21] derived a new phase-space distribution where the radial distribution is exact and the momentum distribution remains close to the quantum provided only that the target electron has a velocity $v_e < 9$. Using this distribution, the ionization cross sections are improved, but there is little change to the charge-exchange results [17,22]. Since our interest here is exclusively with the latter, we have used the "regular" microcanonical distributions in all our calculations. As we approach threshold, the CTMC is at its weakest as it does not recognize the sharp quantum thresholds and has no way of including tunneling effects, and we need to choose a very large initial distance (very small γ). We see that at its lowest energies our results peak and begin to fall away from experiment; we suspect that this is primarily due to the absence of tunneling in our calculations [23]. The orbit of the positron will be fragile compared to that of the much more massive proton, and consequently, one could reasonably assume that at the lowest energy it will not be able to get close enough for tunneling to become significant. Problems still exist in that the approach will not recognize the correct quantum threshold. We have attempted to rectify this by shifting the origin; that is, we assume that the impact energy in the code E_{code} is related to the real impact energy by

$$E = E_{\text{code}} + E_{\text{threshold}}, \tag{7}$$

where $E_{\text{threshold}}$ is the quantum threshold. Further, as we approach threshold, the problem we discussed in Sec. II B of numerical violation of energy conservation becomes more pronounced. We will denote our calculations with both the threshold correction and with (3) enforced by CTMCc to distinguish it from the regular CTMC where neither correction is applied. In Fig. 2 we show both CTMCc and CTMC. For these energies the threshold correction is entirely insignificant, but we do see an effect due to energy nonconservation which becomes progressively more evident as the energy gets smaller; indeed, it becomes unmanageable below about 20 keV, and we were forced to stop our CTMCc calculations at the very lowest energies.

In Fig. 3 we show our CTMCc calculations compared with the experiment of Zhou *et al.* [24]. Agreement is encouraging in that the calculations are consistent with experimental measurements of the absolute magnitude and position of the peak in the cross section. These results are a distinct improvement over the CTMC calculations. Again, as we lowered the impact energy, constraining the energy conservation problem became progressively more difficult.

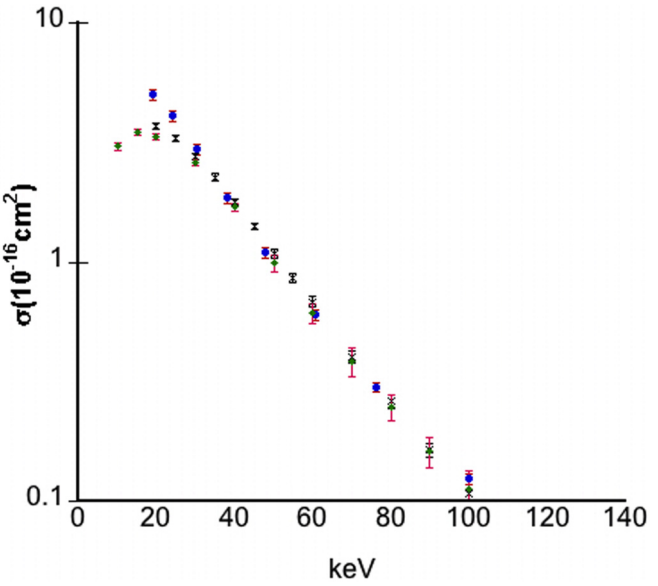

FIG. 2. (Color online) Charge-exchange cross sections for proton collisions with neutral hydrogen: our theoretical calculations, CTMCc with (3) enforced (crosses), and CTMC without threshold correction and where (3) was not enforced (solid diamonds) compared with the absolute experimental data of [20] (solid circles).

B. Helium

The CTMC as we formulated it is obviously restricted to one-electron targets. To calculate the cross section for a multielectron target we need a strategy for closed-shell targets. For reasons of consistency and to retain the mathematical validity of the microcanonical distribution we want to treat the target as a one-electron atom. Our philosophy differs from that of Reinhold and Falcón [25], who extended the classical microcanonical distribution to a two-electron target, used this

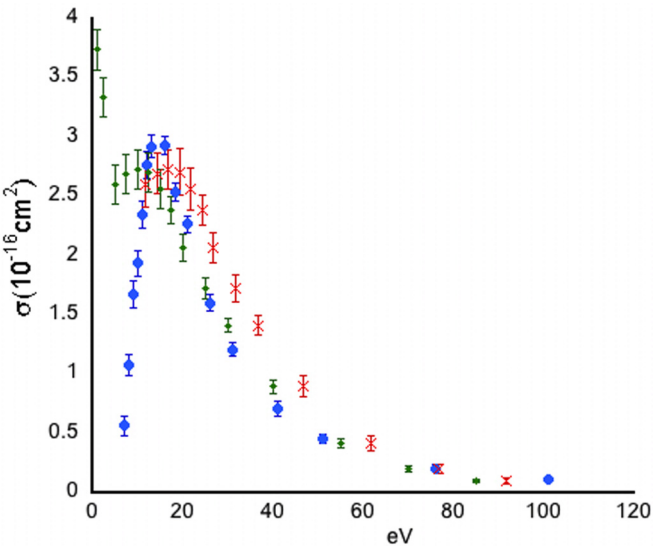

FIG. 3. (Color online) Charge-exchange cross sections for positron collisions with neutral hydrogen: CTMCc (crosses) and CTMC (solid diamonds) compared with the absolute experimental data of [24] (solid circles).

distribution to define the initial conditions for their orbits, and adjusted the potential that the active electron sees. Our approach is to treat the target as a one-electron atom with an effective Coulomb potential:

$$V_{\text{effective}} = \frac{\bar{Z}}{r}.$$

We are concerned with not only getting a good representation of the momentum distribution in the atom but also including something of the response of the two-electron system to the incoming charge. An electron in the n,l,m state of a hydrogenic atom of charge $\bar{Z}$ has a wave function (see, for example, [26])

$$\psi_{nlm}(\mathbf{r}) = R_{nl}(r)Y_l^m(\theta,\phi),$$

where for the ground state, (1,0,0) in atomic units,

$$R_{10}(r) = 2(\bar{Z})^{\frac{3}{2}}e^{-\bar{Z}r}, \quad Y_{00} = \frac{1}{\sqrt{4\pi}}. \tag{8}$$

The wave function in momentum space is then

$$\begin{aligned}\phi_{1,0,0}(\mathbf{p}) &= \frac{1}{(2\pi)^{\frac{3}{2}}}\int e^{-i\mathbf{p}}\psi_{1,0,0}(\mathbf{r})d^3r \\ &= \frac{2^{\frac{3}{2}}}{\pi}\bar{Z}^{\frac{5}{2}}\left[\frac{1}{(\bar{Z}^2+p^2)^2}\right].\end{aligned} \tag{9}$$

It will be convenient to write $\mathbf{p}$ in spherical polar coordinates (p,θ_p,ϕ_p); then the wave function in momentum space may be decomposed [26]:

$$\phi_{nlm}(\mathbf{p}) = F_{nl}(p)Y_l^m(\theta_p,\phi_p). \tag{10}$$

A general formula for $F_{nl}(p)$ is given in [26]. For the ground state we have

$$F_{10}(p) = \frac{(2\bar{Z})^{\frac{5}{2}}}{\sqrt{\pi}}\left[\frac{1}{(\bar{Z}^2+p^2)^2}\right], \tag{11}$$

in agreement with (9). The probability that the absolute value of the momentum lies between p and $p+dp$, independent of direction, is

$$|F_{nl}(p)|^2p^2dp. \tag{12}$$

We can interpret

$$\rho(p) = p^2|F_{nl}(p)|^2 \tag{13}$$

as the momentum distribution. Indeed (see [26]),

$$\int_0^\infty |F_{nl}(p)p|^2dp = 1. \tag{14}$$

We can determine $\bar{Z}$ by deducing it from the static dipole polarizability [26],

$$\bar{\alpha} \equiv 2\sum_{nlm}\frac{|\langle\psi_{nlm}|z|\psi_{1,0,0}\rangle|^2}{E_n - E_1}. \tag{15}$$

For hydrogen $\bar{Z} = 1$, and there is an exact analytic solution of $\bar{\alpha}$ [27], viz., $\bar{\alpha}_H = 4.5$. For a general hydrogenic ion [26]

$$\bar{\alpha}_{\bar{Z}} = \frac{4.5}{\bar{Z}^4}. \tag{16}$$

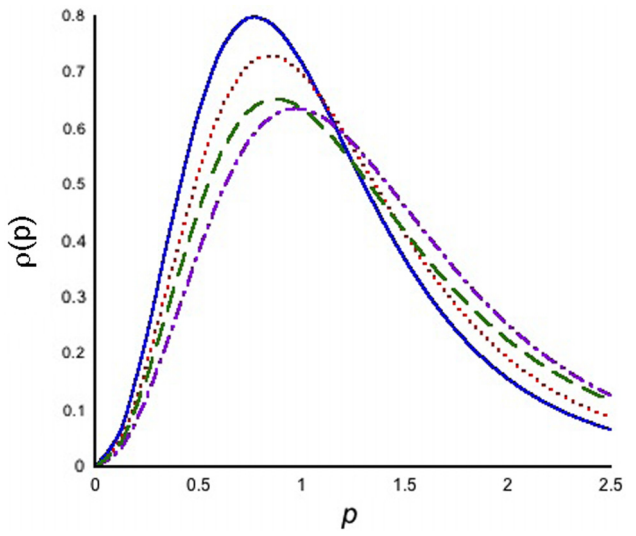

FIG. 4. (Color online) Plot of $p^2|F_{10}(p|^2)$ for hydrogenic ions against the magnitude of the momentum p for various values of $\bar{Z}$ as well as the equivalent Byron-Joachain momentum distribution for helium: $\bar{Z} = 1.344$, solid line; $\bar{Z} = 1.47$, dotted line; $\bar{Z} = 1.6875$, dash-dotted line; Byron-Joachain, dashed line.

Experiment and theory [28] would suggest that the best estimate of the static dipole polarizability of helium is $\bar{\alpha}_{He} = 1.383$ a.u. As a first guess for $\bar{Z}$ we could try

$$\bar{Z} = \left(\frac{\alpha_H}{\alpha_{He}}\right)^{1/4} \approx 1.343 \text{ a.u.} \tag{17}$$

If we take $\bar{Z} = 1.344$, the binding energy of the hydrogenic ion $\frac{\bar{Z}^2}{2}$ will be exactly 24.59 eV [29], the ionization energy of the helium atom, and the polarizability is then 1.379, which is close enough to the current best estimate for helium to lie within the predicted uncertainty. In Fig. 4 we show a comparison between the momentum distribution, (13), with $\bar{Z} = 1.344$ and several other choices. Clement and Raimondi [30] suggest $\bar{Z} = 1.6875$ is a good effective charge to represent the combined field as seen by a helium electron after including the effect of the screening of the nucleus by the other electron. This choice of $\bar{Z}$ corresponds essentially to the energy required to remove two electrons, i.e.,

$$\Delta E = 24.56 \text{ eV} + 54.4 \text{ eV} = 78.96 \text{ eV}.$$

If we treat both electrons as being entirely independent electrons with bound energies $\bar{Z}^2$, then

$$2\bar{Z}^2 = \frac{78.96}{13.6} \Rightarrow \bar{Z} \approx 1.7.$$

We would like our effective charge to give us a reasonable estimate of the binding energy and the polarizability but at the same time to have something of the character of the momentum distribution in the helium atom.

As a wave function for the helium ground state we considered the correlated wave function of Byron and Joachain [31] and the Roothan-Hartree-Fock wave function of [32]. The Byron-Joachain wave function gives a good estimate of the correlation energy, coming within 0.4% of the "exact" value. Interestingly, it is the product of two one-electron wave

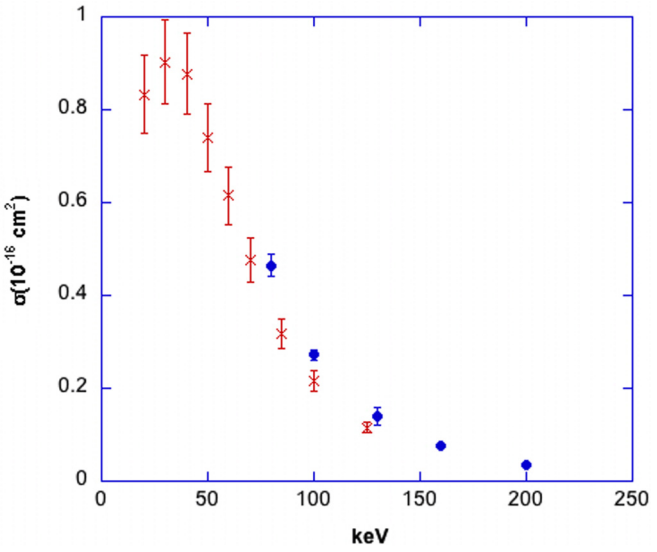

FIG. 5. (Color online) Charge-exchange cross sections for proton collisions with neutral helium: CTMC (crosses) compared with the absolute experimental data of [35] (solid circles).

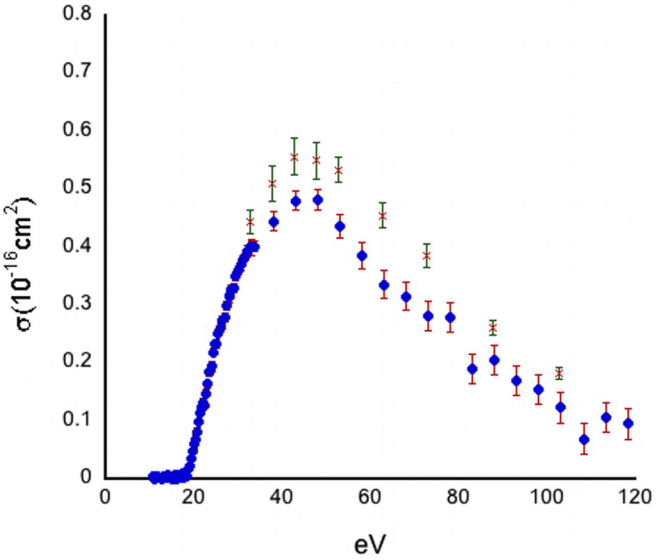

FIG. 6. (Color online) Positronium-formation cross sections for positron collisions with neutral helium: threshold-corrected CTMC ($\bar{Z} = 1.47$; crosses) compared with the absolute experimental data of [11,36] (solid circles).

functions:

$$\phi_0(\mathbf{r}) = \frac{1}{\sqrt{4\pi}}(2.60505e^{-1.41r} + 2.08144e^{-2.61r}), \quad (18)$$

which suggests a crude interpretation of one electron being, on average, more tightly bound than the other. A similar but much more pronounced effect is seen in the representation of the wave functions for negative ions such as H^- [33,34]. In Fig. 4 we show the momentum distribution, (13), for several choices of $1.344 \leqslant \bar{Z} \leqslant 1.6875$ and the equivalent density for helium calculated using the correlated wave function of Byron and Joachain [31]. Calculations using the Roothan-Hartree-Fock wave function of [32] are imperceptibly different from the Byron-Joachain case. The choice $\bar{Z} = 1.6875$ gives the best fit to the distribution but the largest error in the binding energy. Choosing $\bar{Z} = 1.344$ gives the best binding energy and the worst momentum distribution. As a compromise we have chosen to restrict the error in the binding energy to be at most 20%, and this leads us to a choice of $\bar{Z} = 1.47$.

Note that for reasons of consistency and to preserve the validity of the microcanonical distribution we use the theoretical binding energy that corresponds to our choice of $\bar{Z}$ in the CTMC calculations and in (7). In Fig. 5 we show a comparison between our CTMC calculation and experiment for proton impact, and while agreement is good for the range of values where a comparison is possible, we note that our calculations exhibit the same qualitative behavior as we saw for hydrogen with a low-energy peak, so tunneling effects might well increase the cross section in this region. Our threshold-corrected CTMC calculations are in reasonable agreement with experiment for the positron case (Fig. 6). Again the peak position is well predicted, but the absolute magnitude at the peak is a little elevated above experiment.

The analysis of positronium-formation experiments is complicated by the possibility of electron capture into excited states [37]. Because of its classical nature the CTMC does not yield any information as to which quantum state of the positronium the electron is captured into. To estimate this we follow the method outlined in [38]. We calculate the binding energy $U = -E$ and assign a "classical principal quantum number" n_c according to

$$U = \frac{1}{2n_c^2} \text{ a.u.} \quad (19)$$

The classical values are then "quantized" to a specific n level if

$$\left[(n-1)\left(n-\frac{1}{2}\right)n\right]^{\frac{1}{3}} \leqslant n_c \leqslant \left[(n+1)\left(n+\frac{1}{2}\right)n\right]^{\frac{1}{3}}. \quad (20)$$

For positron-hydrogen collisions both fully quantum-mechanical [39] and CTMC calculations [10] find that capture is almost exclusively into the $n = 1$ state, while for Cs both quantum and CTMC predict significant capture into excited states [10,40]. For helium our current calculations show that for threshold-corrected impact energies of less than 42 eV there is essentially 100% capture into $n = 1$. As the impact energy is increased, we see some small amount of capture into excited states; for example, at 100 eV, approximately 85% is captured into $n = 1$, 11% into $n = 2$, 4% into $n = 3$, and 1% into $n = 4$ and little or nothing into higher-lying states. This is in stark contrast to the Cs case where Kernoghan *et al.* [40] estimated for low-energy positron collisions that 20% of the cross section came from $n \geqslant 4$.

C. He^+

Finally, we calculated the CTMC charge-exchange cross section for singly ionized helium.

In Fig. 7 we show a comparison between the CTMCc calculations and experiment for a proton on He^+. While the position and the absolute magnitude of the peak in the experimental data are reasonably well represented, the theoretical distribution is somewhat too broad. It is striking

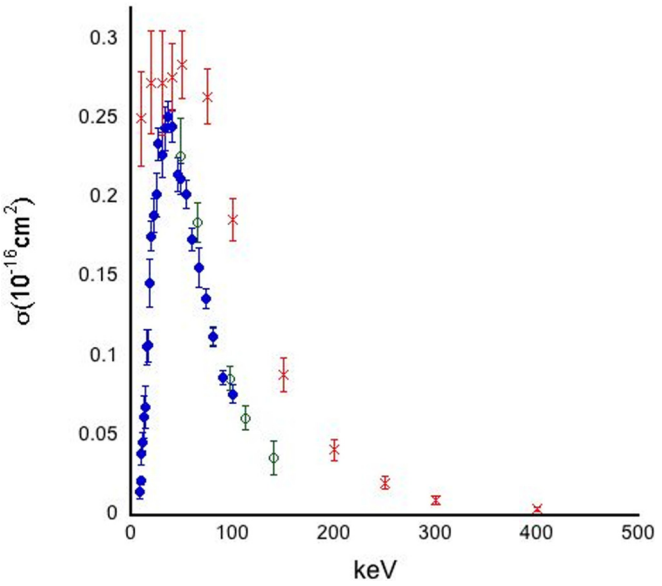

FIG. 7. (Color online) Charge-exchange cross sections for proton collisions with He^+: CTMC (crosses) compared with the absolute experimental data of [41] (solid circles) and [42] (open circles).

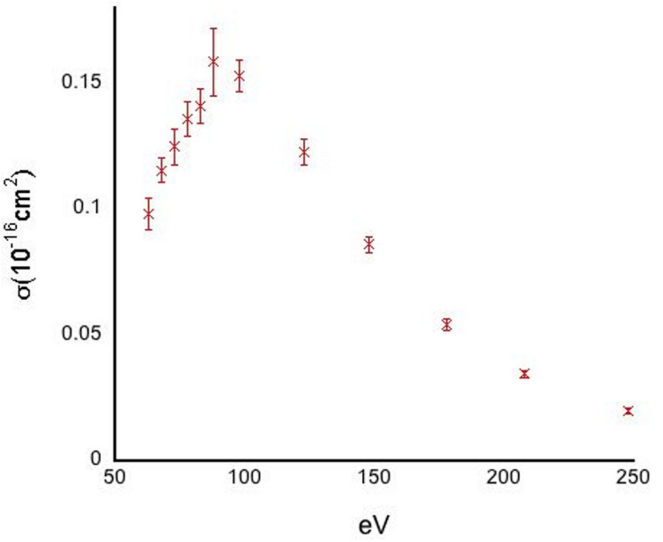

FIG. 8. (Color online) Positronium-formation cross sections for positron collisions with He^+ in the threshold-corrected CTMC (crosses).

that these results are not as good as those we found for proton a on H. Intuitively, one would imagine that the CTMC method would work well for hydrogenic ion targets. The weakness in the CTMC was noted in [22] for H^+ and indeed only gets worse if we increase the charge on the hydrogenic target ion [17,43]. It is not immediately obvious why this is. We note that we found it much more difficult to enforce (3) in the H^+ case. The nuclear charge of the target enters into the step length in the Runge-Kutta, and we suspect that this may be the source of the problem. It would be of value to entirely replace the fourth-order Runge-Kutta part of the code with some form of symplectic or conservative integrator [18,19]. We hope to return to this problem in a future publication.

We were, however, sufficiently encouraged that we calculated the threshold-corrected CTMC for a positron on He^+. Results are shown in Fig. 8. As we mentioned earlier, the finite-step-size instability will be slightly worse is this case. The maximum value of our cross section with (3) enforced is roughly 30% larger than that presented in [10]. There are no experimental data available. However, given the agreement we have found with other calculations in this paper, it would seem likely that these results should be reasonably accurate and would be useful as part of a plasma simulation code, which, after all, is our primary purpose. In Fig. 9 we show a comparison between a fit to the experimental data [36] for a positron on neutral helium and a fit to our CTMC calculation for He^+. Consider a helium plasma containing both neutral and singly ionized helium into which a positron beam is fired. For impact energies less than 17.8 eV there will be no positronium formed. Between 17.8 and 47.6 eV positronium formation will come exclusively from collisions with neutral helium. At energies above 47.6 eV it becomes energetically possible for collisions with ionized helium to contribute, and by 150 eV the contribution from the ion will be at least an order of magnitude bigger than that from the neutral target.

Given our results, it should be possible to construct a model to relate the γ-ray spectrum observed after injecting positrons into a helium plasma to the charge state of the plasma.

IV. CONCLUSIONS

We used the classical trajectory Monte Carlo method to calculate charge-exchange cross sections for positron collisions with hydrogen and neutral and singly ionized helium targets with the ultimate purpose of including these results

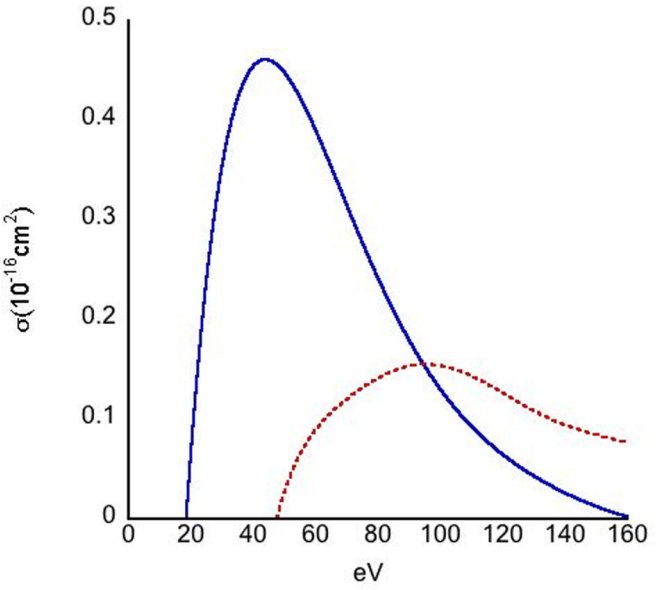

FIG. 9. (Color online) Positronium-formation cross sections for positron collisions with neutral and singly ionized helium: solid blue curve, high-order polynomial fit to the absolute experimental data of [11,36] for neutral helium; dashed red curve, high-order polynomial fit to our CTMC calculations for He^+.

in plasma simulations. We benchmarked these results by comparison with experiment where available and by using the same method to calculate proton collisions with the same targets. We were encouraged by the agreement we found. The CTMC method remains a useful way of estimating charge-exchange cross sections; however, it is important to keep careful track of the errors inherent in the code, and it is misleading to present results without at least displaying the statistical errors. Further for the low-energy positron collisions we found that the numerical integration using the standard fourth-order Runge-Kutta gave rise to a numerical violation of energy conservation, and the containment of this error placed a limit on how small an impact energy we could reliably treat. We hope to return to this problem later.

ACKNOWLEDGMENTS

We are grateful to Professor Gaetana Laricchia for supplying us with her experimental data. This work was performed under the auspices of the Department of Energy by the Lawrence Livermore National Laboratory under Contract No. AC52-07NA-27344. The authors acknowledge support from LLNL's Institute for Laser Science Applications (ILSA).

[1] N. Guessoum, P. Jean, and W. Gillard, Astronomy & Astrophysics **436**, 171 (2005).
[2] N. Prantzos *et al.*, Rev. Mod. Phys. **83**, 1001 (2011).
[3] P. A. Milne, New Astron. Rev. **50**, 548 (2006).
[4] B. L. Brown and M. Leventhal, Astrophys. J. **319**, 637 (1987).
[5] S. C. Ellis and J. Bland-Hawthorn, Astrophys. J. **707**, 457 (2009).
[6] C. J. Crannell, G. Joyce, R. Ramatay, and C. Werntz, Astrophys. J. **210**, 582 (1976).
[7] H. Chen, S. C. Wilks, J. D. Bonlie, E. P. Liang, J. Myatt, D. F. Price, D. D. Meyerhofer, and P. Beiersdorfer, Phys. Rev. Lett. **102**, 105001 (2009).
[8] Hui Chen *et al.*, Rev. Sci. Instrum. **83**, 10E113 (2012).
[9] G. Sarri *et al.*, arXiv:1312.0211 [physics.plasma-ph].
[10] T. C. Naginey, B. B. Pollock, E. W. Stacy, H. R. J. Walters, and C. T. Whelan, Phys. Rev. A **89**, 012708 (2014).
[11] G. Laricchia *et al.*, in *Fragmentation Processes*, edited by C. T. Whelan (Cambridge University Press, Cambridge, 2013), p. 116.
[12] R. Abrines and I. C. Percival, Proc. Phys. Soc. **88**, 861 (1966).
[13] R. Abrines and I. C. Percival, Proc. Phys. Soc. **88**, 873 (1966).
[14] D. Banks *et al.*, Comput. Phys. Commun. **13**, 251 (1977).
[15] R. E. Olson, in *Atomic, Molecular and Optical Physics Handbook*, edited by D. W. F. Drake (AIP, New York, 1996), p. 664.
[16] V. A. Fock, Bull. Acad. Sci. USSR **2**, 169 (1935).
[17] B. H. Bransden and M. R. C. McDowell, *Charge Exchange and the Theory of Ion-Atom Collisions* (Oxford University Press, Oxford, 1992).
[18] B. Leimkuhler and S. Reich, *Simulating Hamiltonian Dynamics* (Cambridge University Press, Cambridge, 2005).
[19] O. Kotovych and J. C. Bowman, J. Phys. A **35**, 7849 (2002).
[20] G. W. McClure, Phys Rev **148**, 47 (1966).
[21] J. S. Cohen, J. Phys. B: At. Mol. Phys. **18**, 1759 (1985).
[22] C. O. Reinhold and C. A. Falcon, J. Phys. B: At. Mol. Phys. **21**, 2473 (1988).
[23] S. Keller, H. Ast, and R. M. Dreizler, J. Phys. B: At. Mol. Phys. **26**, L737 (1993).
[24] S. Zhou, H. Li, W. E. Kauppila, C. K. Kwan, and T. S. Stein, Phys. Rev. A **55**, 361 (1997).
[25] C. O. Reinhold and C. A. Falcón, Phys. Rev. A **33**, 3859 (1986).
[26] B. H. Bransden and C. J. Joachain, *Physics of Atoms and Molecules*, 2nd ed. (Prentice Hall, Harlow, 2003).
[27] A. Dalgarno and J. T. Lewis, Proc. R. Soc. London Ser. A **233**, 70 (1955).
[28] M. Masili and A. F Starace, Phys. Rev. A **68**, 012508 (2003).
[29] http://dept.astro.lsa.umich.edu/~cowley/ionen.htm.
[30] E. Clement and D. L. Raimondi, J. Chem. Phys. **38**, 2686 (1963).
[31] F. W. Byron, Jr., and C. J. Joachain, Phys. Rev. **146**, 1 (1966).
[32] E Clementi and C Roetti, At. Data Nucl. Data Tables **14**, 177 (1974).
[33] S. Lucey *et al.*, J. Phys. B: At. Mol. Phys. **29**, L489 (1996).
[34] D. P. Dewangen and H. R. J. Walters, J. Phys. B: At. Mol. Phys. **11**, 3983 (1978).
[35] M. B. Shah and H. B. Gilbody, J. Phys. B: At. Mol Phys. **18**, 899 (1985).
[36] D. J. Murtagh *et al.*, J. Phys. B: At. Mol. Phys. **38**, 3857 (2005).
[37] G. Laricchia *et al.*, J. Phys. B: At. Mol. Phys. **35**, 2525 (2002).
[38] R. E. Olson, Phys. Rev. A **24**, 1726 (1981).
[39] A. A. Kernoghan *et al.*, J. Phys. B: At. Mol. Opt. Phys. **29**, 2089 (1996).
[40] A. A. Kernoghan, M. T. McAlinden, and H. R. J. Walters, J. Phys. B **29**, 3971 (1996).
[41] K. Rinn, F. Melchert, and E. Salzborn, J. Phys. B: At. Mol. Phys. **18**, 3783 (1985).
[42] M. F. Watts, K. F. Dunn, and H. B. Gilbody, J. Phys. B: At. Mol. Phys. **19**, L355 (1986).
[43] A. M. Ermolaev, B. H. Bransden, and C. R. Mandel, Phys. Lett. A **125**, 44 (1987).